

Optimized Atom Interferometer Design Including van der Waals Interactions

Alexander D. Cronin, Lu Wang, John Perreault

Department of Physics, University of Arizona, 1118 E 4th St. Tucson, Arizona 85721

(Dated: April 7, 2005)

The problem of designing an atom interferometer with optimum sensitivity to de Broglie wave phase shifts is revisited. Because van der Waals interactions affect how efficiently material gratings work as beam splitters, we find the optimum open fraction for each of the gratings in a three-grating Mach Zehnder atom interferometer depends on the van der Waals interaction strength as well as the atom velocity and grating period.

PACS numbers:

Keywords:

Atom interferometers built with nanostructure gratings have been used for to measure Na atomic polarizability [1], the index of refraction for atomic matter waves due to a dilute gas [2, 3], the laboratory rotation rate [4], and the strength of atom-surface van der Waals interaction potentials [5]. All of these measurements are accomplished by determining the phase shift of interference fringes. Therefore, one of the important design goals for atom interferometers is to optimize sensitivity to the phase of an interference pattern. This goal has been discussed by Schmiedmayer et al. in their contribution to the book “Atom Interferometry” [6] and also by the group of Vigué in references [7, 8] for interferometers based on mechanical gratings. In this paper we recall how phase sensitivity is maximized by selecting the open fraction of each grating, and then discuss modifications due to atom-surface van der Waals interactions.

The van der Waals interaction between atomic de Broglie waves and the material grating bars changes the *diffraction efficiencies*, i.e the amplitude in each diffraction order with respect to the incident amplitude, as has been shown in [9–12]. Here we show that atom-surface interactions can reduce the performance of an interferometer. The statistical precision for phase shifts is reduced to $\frac{3}{4}$ for an interferometer built using a sodium atom beam with a mean velocity of 1000 m/s and 100-nm period, 150-nm thick, silicon nitride gratings unless the open fractions of the gratings are enlarged over previous design values. Considering the possibility of smaller gratings, such as 33-nm period gratings with 50 nm thickness (one third the scale of the gratings presently in use), the statistical precision in measured phase would be reduced by a factor of $\frac{1}{3}$ unless van der Waals interactions are included in the procedure for optimizing the grating open fractions as described here.

The layout of an atom beam interferometer with separated beams is shown in Figure 1. The first grating serves (G1) as a beam splitter. The second grating (G2) redirects the beams so they overlap in space and make a flux density interference pattern. The third grating (G3) serves as a mask so that the transmitted flux $I(x_3)$

depends on position of the third grating, x_3 , as

$$I(x_3) = \langle I \rangle [1 + C \cos(k_g x_3 + \phi)] \quad (1)$$

where $\langle I \rangle$ is the average atom beam intensity, C is the contrast defined as

$$C = \frac{I_{\text{Max}} - I_{\text{Min}}}{I_{\text{Max}} + I_{\text{Min}}}, \quad (2)$$

k_g is the wavenumber of the grating, and ϕ is the phase that the interferometer is designed to measure. Example of interference fringe data and a best fit curve with $\langle I \rangle$, C , and ϕ as free parameters are shown in Figure 2. The period d is the same for all three gratings, and the distance x_3 is independently measured.

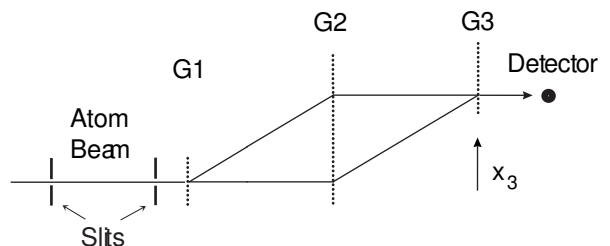


FIG. 1: Interferometer layout. G1, G2 and G3 are the three gratings. x_3 is the position of the third grating.

The Intensity, $I(x_3)$, multiplied by the detector area and detector efficiency yields the predicted atom count rate. The count rate multiplied by the duration of detection gives the predicted number of atoms $N(x_3)$ counted when the third grating is located in the range of position x_3 to $x_3 + dx_3$. The range dx_3 is a parameter chosen for the data analysis so there are at least 10 bins per fringe. Assuming Poisson statistics in the count rate for atoms, the RMS variation in $N(x_3)$ is $\sqrt{N(x_3)}$. This determines the error bars shown for each data point in Figure 2. As discussed in [6], the statistical uncertainty in the phase is

$$\sigma_\phi = \frac{1}{C\sqrt{N}} \quad (3)$$

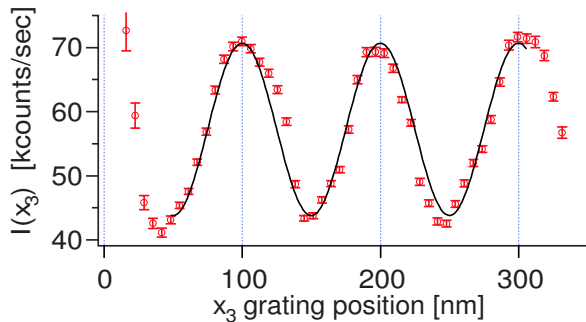


FIG. 2: Interference fringe data and best fit based on Equation 1. $\langle I \rangle = 57,000$ counts per second, and $C = 0.23$. A total of 4 seconds of data are shown and the uncertainty in phase is $\sigma_\phi = .01$ radians.

where N is the total number of atoms counted in all position bins combined. To minimize σ_ϕ we therefore seek to maximize the quantity $C\sqrt{\langle I \rangle}$ by choosing three gratings with specific open fractions. The open fractions are defined as w_i/d where w_i is the size of the grating window for the i th grating (G1 G2 or G3) and d is the grating period.

ANALYSIS OF G3 AS A MASK

Since the third grating acts as a mask, it attenuates the intensity and reduces the contrast of the interference pattern formed in space just before the third grating. The atom flux density just before the third grating is given by an equation similar to Eq. 1,

$$I'(x') = \langle I' \rangle [1 + C' \cos(k_g x' + \phi)] \quad (4)$$

where the primes indicate the position, average intensity and contrast of the interference pattern before the third grating. The transmitted intensity is given by

$$I(x_3) = \frac{1}{d} \int_{-w_3/2}^{w_3/2} I'(x_3 - x') dx' \quad (5)$$

where w_3 is the window size of the third grating, and d is the grating period. The ratio w_3/d defines the open fraction for the third grating. The result of the integral in Equation 5 is

$$I(x_3) = \langle I' \rangle \frac{w_3}{d} \left[1 + C' \frac{\sin(k_g w_3/2)}{(k_g w_3/2)} \cos(k_g x_3 + \phi) \right]. \quad (6)$$

This lets us identify

$$\langle I \rangle = \frac{w_3}{d} \langle I' \rangle, \quad (7)$$

and

$$C = \frac{\sin(k_g w_3/2)}{(k_g w_3/2)} C'. \quad (8)$$

Regardless of the values of C' and $\langle I' \rangle$, we can maximize the product $C\sqrt{\langle I \rangle}$ by requiring

$$\frac{d}{dw_3} \left[\frac{\sin(k_g w_3/2)}{\pi \sqrt{w_3/d}} \right] = 0 \quad (9)$$

This makes the optimum w_3 at the value for which

$$w_3 k_g = \tan(w_3 k_g/2). \quad (10)$$

In the range $0 < w_3 < d$ there is only one solution, and this is $w_3 = 0.37 \times d$. This reproduces the result in [6].

ANALYSIS OF G1 & G2 WITHOUT VDW

If van der Waals interactions with the grating bars are ignored, the diffraction efficiency for atom wave amplitude into the n th transmission diffraction order is given by

$$e_n \equiv \frac{\Psi_n}{\Psi_{inc}} = \left(\frac{w}{d} \right) \frac{\sin(n\pi w/d)}{(n\pi w/d)} \quad (11)$$

where Ψ_{inc} is the incident atom wave amplitude, w is the grating window size and d is the grating period. This makes the familiar diffraction envelope function for diffraction order intensities I_n :

$$(e_n)^2 = \frac{I_n}{I_{inc}} = \left(\frac{w}{d} \right)^2 \frac{\sin^2(n\pi w/d)}{(n\pi w/d)^2} \quad (12)$$

where I_{inc} is the incident intensity. We shall denote the diffraction efficiency for amplitudes into the n th order from grating G1 by the notation e_n^{G1} .

The interference pattern just before the third grating is determined by

$$I'(x') = \left| e_0^{G1} e_1^{G2} + e_1^{G1} e_{-1}^{G2} e^{i(k_g x' + \phi)} \right|^2 I_{inc}. \quad (13)$$

After the third grating, the average intensity is

$$\langle I \rangle = \left[(e_0^{G1} e_1^{G2})^2 + (e_1^{G1} e_{-1}^{G2})^2 \right] \left[\frac{w_3}{d} \right], \quad (14)$$

and the contrast is

$$C = \frac{e_0^{G1} e_1^{G2} e_1^{G1} e_{-1}^{G2}}{(e_0^{G1} e_1^{G2})^2 + (e_1^{G1} e_{-1}^{G2})^2} \left[\frac{\sin(k_g w_3/2)}{(k_g w_3/2)} \right]. \quad (15)$$

The last factor in brackets is 0.790 when $w_3/d = .37$. This analysis assumes that the detector is small enough to resolve the paths shown in Figure 1, but large enough to collect the entire width of each beam. Furthermore, the location of the detector is assumed to be close to G3 so that we may ignore diffraction from G3.

The quantity we seek to maximize by choosing the open fractions of G1 and G2, is

$$C' \sqrt{\langle I' \rangle} = \frac{e_0^{G1} e_1^{G2} e_1^{G1} e_{-1}^{G2}}{\sqrt{(e_0^{G1} e_1^{G2})^2 + (e_1^{G1} e_{-1}^{G2})^2}}. \quad (16)$$

Assuming $e_1 = e_{-1}$ for G2, we can simplify this to obtain:

$$C' \sqrt{\langle I' \rangle} = \left(\frac{e_0^{G1} e_1^{G1}}{\sqrt{(e_0^{G1})^2 + (e_1^{G1})^2}} \right) (e_1^{G2}) \quad (17)$$

which has been factored into a part that depends only on G1 times a part that depends only on G2. Each part can then be maximized independently. Using Eq. 11 for the diffraction efficiencies with no van der Waals interaction we can rewrite Eq. 17

$$C' \sqrt{\langle I' \rangle} = \left(\frac{\sin(\frac{\pi w_1}{d})}{\sqrt{\pi^2 + (\frac{w_1}{d})^2 \sin^2(\frac{\pi w_1}{d})}} \right) \left(\frac{\sin(\frac{\pi w_2}{d})}{\pi} \right). \quad (18)$$

Again, this is factored into a function of w_1 and a function of w_2 , and both of these functions can be maximized independently. The first factor is maximized by selecting $w_1/d = 0.557$ as shown in Figure 3(top). The second factor is maximized by selecting $w_2/d = 0.500$ as shown in Figure 3(middle). In this way the window sizes in the absence of van der Waals interactions can be chosen to optimize the figure of merit $C\sqrt{I}$, which is given by the product of the three independent functions shown in Figure 3. In the next section, it will be shown how van der Waals interactions modify these results.

EFFECT OF VDW INTERACTIONS

To predict how the diffraction efficiencies change as a result of the van der Waals (vdW) interaction we used a numerical calculation described in [12] and briefly summarized here. The van der Waals potential is

$$V(r) = -\frac{C_3}{r^3}, \quad (19)$$

where r is the distance to an infinite plane and C_3 is the *vdW coefficient*. The vdW coefficient for sodium atoms and silicon nitride surfaces has been measured to be $C_3 = 3 \text{ meVnm}^3$ [11]. The phase shift for atom waves passing through the grating channel between two bars as given in [11, 12] is approximately

$$\phi(\xi) = \frac{C_3 \ell}{\hbar v} \left(\frac{1}{|\xi - w/2|^3} + \frac{1}{|\xi + w/2|^3} \right) \quad (20)$$

where ξ is the coordinate inside the grating channel ($\xi = 0$ in the middle of the window), ℓ is the thickness of the grating, i.e. the distance atoms travel in the potential, \hbar is Planck's constant divided by 2π , and v is the mean atom beam velocity. With this vdW induced phase shift, the diffraction efficiencies are

$$e_n \equiv \frac{|\Psi_n|}{|\Psi_{inc}|} = \frac{1}{d} \int_{-w/2}^{w/2} e^{i(nk\xi + \phi(\xi))} d\xi. \quad (21)$$

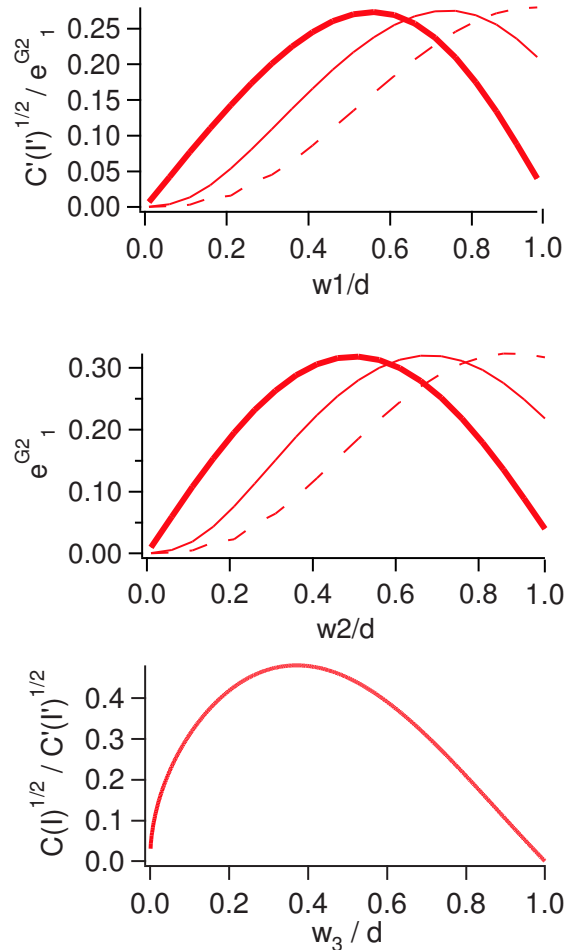


FIG. 3: The optimization of $C\sqrt{I}$ by selection of w_1 , w_2 , and w_3 in the absence of vdW interactions. (Top) The first factor in Eq. 17 is determined by w_1 . (Middle) The second factor in Eq. 17 is determined by w_2 . (Bottom) The ratio $C\sqrt{I}/C'\sqrt{I'}$ from Eq.s 7 and 8 is determined by w_3 . The thick solid curves correspond to $C_3=0$. The thin solid curves correspond to $C_3 = 3 \text{ meVnm}^3$, and the dashed curves correspond to $C_3 = 30 \text{ meVnm}^3$ and each case is for velocity $v = 1000 \text{ m/s}$, and grating period $d = 100 \text{ nm}$ and grating thickness $\ell = 150 \text{ nm}$.

It can be shown from Eq.s 20 and 21 that the efficiencies now depend on two independent parameters

$$e_n = e_n \left(\frac{w}{d}, \frac{C_3 \ell}{vd^3} \right). \quad (22)$$

This permits us to show how the efficiencies scale with atom velocity, grating period, and atom-surface van der Waals coefficient C_3 . Using for the specific examples square grating bars with $d=100 \text{ nm}$, and $\ell = 150 \text{ nm}$, and atoms with velocity $v=1000 \text{ m/s}$, we computed how the figure of merit changes with the van der Waals potential strength C_3 in Figure 4. This prediction is made for three sets of window sizes that are chosen to maximize $C\sqrt{I}$ for $C_3 = 0, 3$, and 30 as shown in Table I.

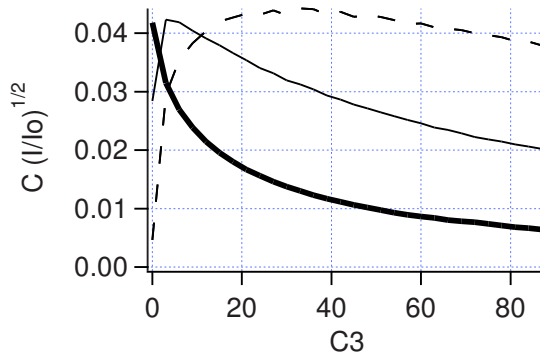


FIG. 4: The figure of merit for phase sensitivity vs. the van der Waals potential coefficient C_3 . Predictions are shown for open fractions (0.57, 0.50, 0.37) in thick solid curve, (0.75, 0.67, 0.37) in thin solid curve and (0.93, 0.88, 0.37) dashed solid curve.

TABLE I: Figures of merit tabulated for various open fractions for G1 and G2 given different values of C_3 (in units of meVnm^3) assuming the grating period $d = 100$ nm and the atom velocity is $v = 1000\text{m/s}$.

C_3	w_1/d	w_2/d	w_3/d	C	$\langle I \rangle / I_{inc}$	$C\sqrt{\langle I \rangle / I_{inc}}$
0	.56	.50	.37	.34	.015	.042 ★
3	.56	.50	.37	.38	.007	.031
3	.75	.67	.37	.33	.016	.042 ■
30	.56	.50	.37	.39	.001	.014
30	.93	.88	.37	.34	.016	.044 ⊗

★ optimized for $C_3 = 0$, equivalent to work in [6].

■ optimized for $C_3 = 3 \text{ meVnm}^3$, the value measured by [11]

⊗ optimized for $C_3 = 30 \text{ meVnm}^3$.

When $C_3 \neq 0$ is included in the design criterion, the G1 and G2 open fractions can be selected to make the value of $C\sqrt{I}$ at least as good as the case when $C_3 = 0$. For non-zero C_3 , larger open fractions are generally preferred for both G1 and G2. This can be understood from the qualitative statement that the vdW interaction generally enhances the higher diffraction orders and reduces the flux into the zeroth order as has been shown in [9–12].

If every geometric dimension of the gratings (d, w , and ℓ) were to be reduced by a factor of p , then by Equation 22 it is evident that the efficiencies e_n would be identical to the present calculations for a value of C_3 increased by p^2 . Therefore, if we could obtain gratings with a 32-nm period (and 47-nm depth) made of the same material that

has a measured $C_3 = 3 \text{ meVnm}^3$, then the diffraction efficiencies and the value for $C\sqrt{I}$ would be equal to those shown in Figures 4 and 3 for $d = 100$ nm using $C_3 = 30$.

In conclusion, now that it has been shown both experimentally and theoretically that atom surface van der Waals interactions modify diffraction efficiencies, we should include this effect when designing an atom interferometer. For example, we have shown that a 1000 m/s sodium atom beam interferometer with 100 nm period silicon nitride gratings would work best if the grating open fractions were chosen to be $(w_1, w_2, w_3) = (0.75, 0.67, 0.37)$. These open fractions are significantly larger than the optimum values found without considering van der Waals interactions. Furthermore, as the grating period is made smaller or the atom velocity is reduced, an even larger set of open fractions is preferred.

This work is supported by grants from Research Corporation and the NSF.

-
- [1] C. Ekstrom, J. Schmiedmayer, M. Chapman, T. Hammond, and D. E. Pritchard, Phys. Rev. A **51**, 3883 (1995).
 - [2] J. Schmiedmayer, M. Chapman, C. Ekstrom, T. Hammond, S. Wehinger, and D. Pritchard, Phys. Rev. Lett. **74**, 1043 (1995).
 - [3] T. D. Roberts, A. D. Cronin, D. A. Kokorowski, and D. E. Pritchard, Physical Review Letters **89** (2002).
 - [4] T. Hammond, M. Chapman, A. Lenef, J. Schmiedmayer, E. Smith, R. Rubenstein, D. Kokorowski, and D. Pritchard, Braz. J. Phys. **27**, 193 (1997).
 - [5] J. D. Perreault and A. D. Cronin, sub to prl (2005).
 - [6] P. R. Berman, ed., *Atom Interferometry* (Academic Press, 1997).
 - [7] C. Champenois, M. Buchner, and J. Vigue, European Physical Journal D **5**, 363 (1999).
 - [8] R. Delhuille, A. Miffre, B. V. de Lesegno, M. Buchner, C. Rizzo, G. Trenec, and J. Vigue, Acta Physica Polonica B **33**, 2157 (2002).
 - [9] R. E. Grisenti, W. Schollkopf, J. P. Toennies, G. C. Hegerfeldt, and T. Kohler, Phys. Rev. Lett. **83**, 1755 (1999).
 - [10] R. Bruhl, P. Fouquet, R. E. Grisenti, J. P. Toennies, G. C. Hegerfeldt, T. Kohler, M. Stoll, and D. Walter, Europhys. Lett. **59**, 357 (2002).
 - [11] J. Perreault, A. Cronin, and T. Savas, arXiv:physics/0312123 (2003).
 - [12] A. Cronin and J. Perreault, Phys. Rev. A **70**, 043607 (2004).